# Effect of Voltage Limiting Device Operation on Rail Potential and Stray Current in DC Railway Systems

Warayut Kampeerawat[1], Jonggrist Jongudomkarn[1], Phumin Kirawanich[2], and Chaiyut Sumpavakup[3,*]

ARTICLE INFO

*Article history:*
Received: 14 December 2021
Revised: 1 February 2022
Accepted: 21 February 2022

*Keywords*:
Voltage limiting devices
Rail potential
DC railway system

ABSTRACT

This paper presents the effect of voltage limiting devices (VLD) operation on the rail potential and stray current in DC railway system. The objective of the study is to simulate and consider the variation in the rail potential and the generated stray current at the VLD installed location while the train is operated under normal conditions. In the study, 3 factors are selected for the simulation i.e., time duration of VLD operation, variation of the running rail resistance, and variation of the ground resistance. According to the simulation results, the operating time of VLD affects the duration of suppressing the rail potential, and the stray current can possibly increase to a surprising value during the VLD operation. The running rail resistance significantly affects the rail potential and stray current. Moreover, the variation in rail resistance may affect the operating time duration when the rail potential exceeds the threshold of VLD. The resistance of ground system has a slight effect on rail potential while it still affects significantly on the stray current.

## 1. INTRODUCTION

Nowadays, DC railway system is an effective transportation for urban area. For the third-rail feeding system and overhead feeding system of DC railway, running rail is typically used as a return path for the current to flow back to the traction power supply. In normal train operation, the rail potential is possibly high at the rail structure as well as other nearby structures. If the rail potential is quite high by somehow, it may be dangerous to operators and passengers [1].

For the safety implications regarding rail potential, therefore, the measures for controlling such the rail potential are set according to the IEC 62128 standard and EN 50122-1 [2, 3]. The rail potential also affects the stray current that occurs between the rail and ground. To limit the rail potential, voltage limiting devices such as MOV and VLD is installed at power stations, passenger stations, or between two sections of the route depending on the purpose of protection. In case of preventing excessive touch voltage, voltage limiting devices are commonly installed at the passenger stations between the running rails and the ground grid system. The variation of rail potential depends on various factors, e.g., rail resistance, ground resistance, train position on the rail, surge voltage from switching operation [4, 5].

Basically, there is leakage current along the railway track called the stray current resulting from imperfection of insulation between rail and support structure. Various studies on stray current monitoring and estimation have been performed to improve the method of stray current reduction and protection [6]-[8]. The safety requirement of stray current is determined based on rail-to-earth resistance to limit leakage current along the track according to the IEC 62128-2 [9].

To determine the rail potential in normal operating conditions, a simulated model of the electrical system of the transmission line, rail, and ground can be considered by means of resistive equivalent circuit. In a simple analysis, a lumped parameter model is used to calculate the voltage at different positions in the system and the rail potential [10]. To study the variation of the rail potential including the distribution of stray current into the ground, a more sophisticated model is required. Considering the relationship of current and voltage in the form of differential equations and using distributed parameters [10]-[14]. Some preceding works presented the results of calculating the rail potential considering the voltage limiting devices installed at the traction substation, but the variation of rail potential and resultant stray current due to the factors relating VLD operation and some variation of system parameters have not been mentioned yet [1, 6, 15].

[1] *Department of Electrical Engineering, Faculty of Engineering, Khon Kaen University,Khon Kaen 40002, Thailand*.
[2] *The Cluster of Logistics and Rail Engineering, Faculty of Engineering, Mahidol University, Nakhon Pathom 73170, Thailand*.
[3] *Research Centre for Combustion Technology and Alternative Energy – CTAE and College of Industrial Technology, King Mongkut's University of Technology North Bangkok, Bangkok 10800, Thailand*.
**Corresponding author:* Chaiyut Sumpavakup; Phone: +66-885-592-351; Email: chaiyut.s@cit.kmutnb.ac.th.

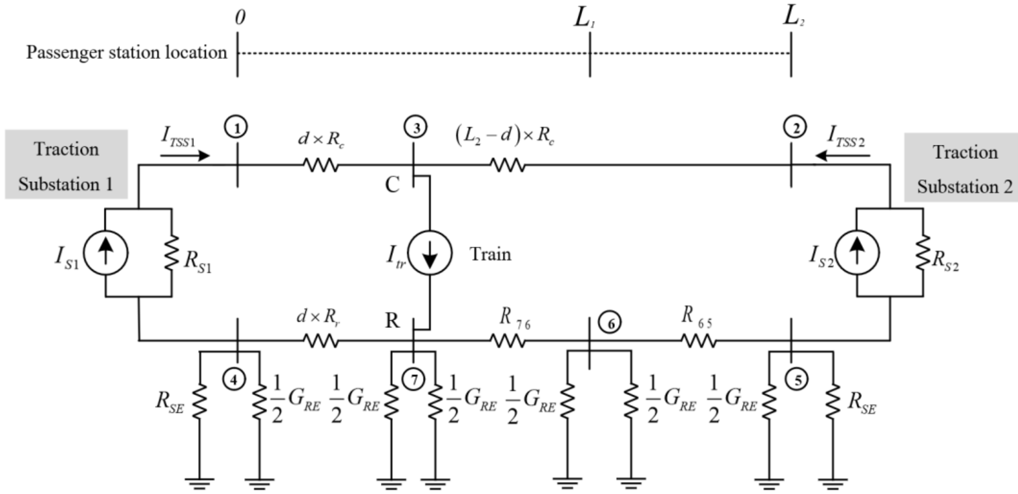


**Fig. 1. Equivalent circuit of DC railway system**

This paper presents the effect of voltage limiting devices operation is installed at the passenger stations to limit the rail voltage in DC railways. An electrical model of railway system with lumped parameters and a simplified model of VLD are used to determine the rail potential and leakage current at the installed location of VLD while the railway is operating in normal conditions. Moreover, the variation of operating time VLD, the variation of rail resistance and grounding resistance are considered and discussed. In section 2, the electrical model and analysis method used for the simulation are described. The numerical results from the simulation with 3 case studies are demonstrated and discussed in section 3. Finally, the study is concluded with the outlook in section 4.

## 2. ANALYSIS OF DC RAILWAY POWER SUPPLY INCLUDING THE VOLTAGE LIMITING DEVICES

In the analysis part, the rail potential and stray current at a specific location are considered, while variation of voltage along rail length and the distribution of current in the ground are ignored. Therefore, the simplified equivalent circuit with lumped parameters shown in Fig.1 [16] is used for analysis to simulate the electrical system of DC railway. In the equivalent circuit, single train is considered to operate on the track and the train load is modeled as a current source. The traction substation is modelled as Norton's equivalent model. Where $d$ is the train position on a rail, $L$ is the passenger station position , $R_C$ and $R_R$ are the conductor rail resistance and the running rail resistance, respectively, $R_S$ is the short-circuit resistance at the traction substation, $I_{TSS}$ is the current at the traction substation, $I_{tr}$ is the train current, $R_{76/65}$ is the resistance between nodes 7 and 6 or nodes 6 and 5, $G_{RE}$ is the rail-to-earth conductance, $R_{SE}$ and $R_E$ are the ground resistance of traction substation and ground resistance at the passenger station, respectively.

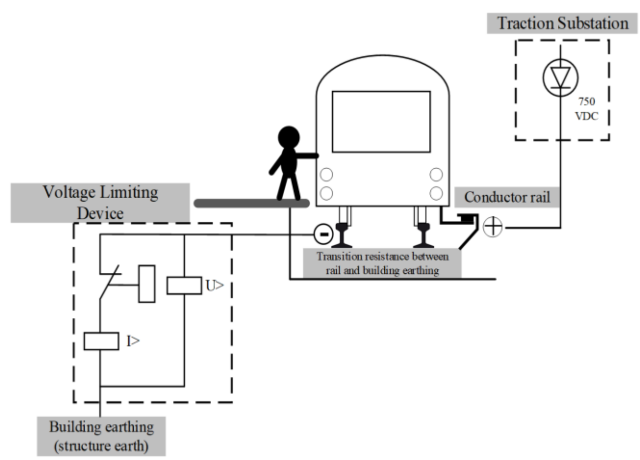


**Fig. 2. Voltage Limiting Device installed at a passenger station.**

Considering a dc railway with the third-rail feeding system, a VLD is installed at a passenger station as shown in Fig.2. VLD is supposed to operate to limit rail potential for safety purpose. The simplified electrical model of VLD is represented by the resistance between the ground system and rail conductor, $R_{VLD}$ is the VLD resistance. Where the $R_{VLD}$ changes according to the conditions in equation (1).

$$R_{VLD} = \begin{cases} 0.001\,\Omega & ;\text{if VLD is ON} \\ 100\ \text{M}\Omega & ;\text{if VLD is OFF} \end{cases} \quad (1)$$

For the calculation of the rail potential including VLD, the equivalent circuit shown in Fig.3 is used. From the circuit, the node voltage can be obtained from solving equations of node analysis and using an iteration computational method. The nodal equations of the circuit with a train moving along the route can be derived as in equation (2).

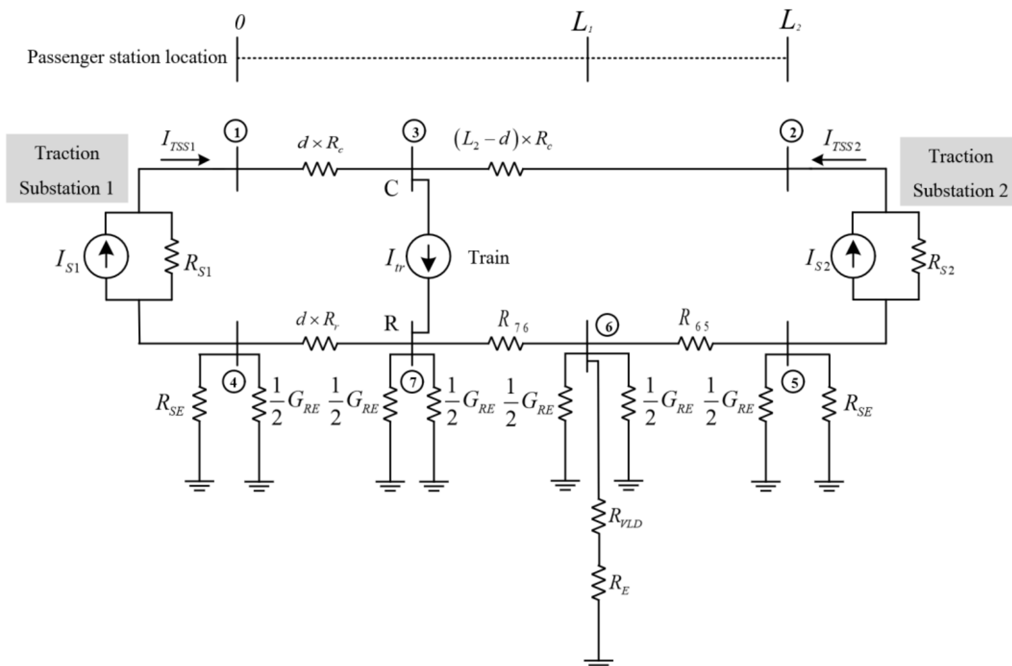


**Fig. 3 Equivalent circuit of DC railway system with Voltage Limiting Device (VLD) installed at a passenger station**

$$I_{node(7\times1)} = G_{node(7\times7)} V_{node(7\times1)} \tag{2}$$

where, $I_{node}$ and $V_{node}$ are the vector of nodal current and voltage, respectively, $G_{node}$ is the nodal conductance matrix. The nodal current can be derived as follows.

$$I_{node(7\times1)} = \begin{bmatrix} I_{TSS1} & I_{TSS2} & -I_{tr} & -I_{TSS1} & -I_{TSS2} & 0 & I_{tr} \end{bmatrix}^T$$

The members of the nodal conductance matrix can be derived as the following.

$$G_{11} = \frac{1}{d\times R_c} + \frac{1}{R_{s1}},\ G_{22} = \frac{1}{(L_2-d)\times R_c} + \frac{1}{R_{s2}},$$

$$G_{33} = \frac{1}{(L_2-d)\times R_c} + \frac{1}{d\times R_c},$$

$$G_{44} = \frac{1}{R_{SE}} + \frac{G_{RE}}{2} + \frac{1}{R_{47}}; R_{47} = \begin{cases} d\times R_r; d < L_1 \\ L_1\times R_r; d \geq L_1 \end{cases},$$

$$G_{55} = \frac{1}{R_{SE}} + \frac{G_{RE}}{2} + \frac{1}{R_{65}}; R_{65} = \begin{cases} (L_2 - L_1)\times R_r; d \leq L_1 \\ (L_2 - d)\times R_r; d > L_1 \end{cases},$$

$$G_{66} = \frac{1}{R_{67}} + \frac{1}{R_{65}} + G_{RE} + \frac{1}{(R_{VLD} + R_E)}; R_{67} = \begin{cases} (L_1 - d)\times R_r; d < L_1 \\ L_1\times R_r; d \geq L_1 \end{cases}$$

$$G_{77} = \frac{1}{R_{47}} + \frac{1}{R_{67}} + G_{RE},\ G_{13} = G_{31} = -\frac{1}{d\times R_c},$$

$$G_{14} = G_{41} = -\frac{1}{R_{s1}},\ G_{23} = G_{32} = -\frac{1}{(L_2-d)\times R_c},$$

$$G_{25} = G_{52} = -\frac{1}{R_{s2}},\ G_{47} = G_{74} = -\frac{1}{R_{47}},\ G_{56} = G_{65} = -\frac{1}{R_{65}},$$

$G_{67} = G_{76} = -\frac{1}{R_{67}}$ and other than those values, $G_{ii} = 0$.

When the train position is changed, the position of node no. 3 and node no.7 will also be changed by the time leading to the change of equivalent circuit. To obtain the train position at each time step, the train movement calculation is performed [16].

## 3. CASE STUDY AND NUMERICAL RESULTS

### *3.1. Test system information*

The test system is composed of 3 passenger stations (Station 1 – Station 3) with the service distance of 2.169 km and 2 DC traction substations. VLD was installed at the Station 2 as shown in Fig. 4. For a simulated condition, a train is operated from Station 1 and stopped at Station 3. The vehicle data and electrical parameters for simulation are listed in Table 1, and the simulation is performed by using MATLAB/M-file software. For the train movement calculation, a train speed profile with its consumed power and tractive/brake effort are shown in Fig. 5, Fig.6 and Fig.7, respectively.

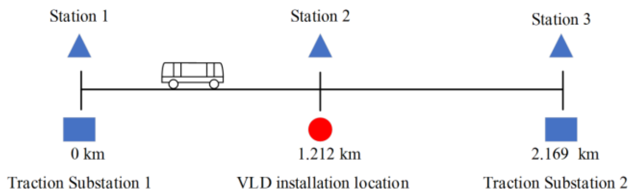


**Fig. 4. Test system.**

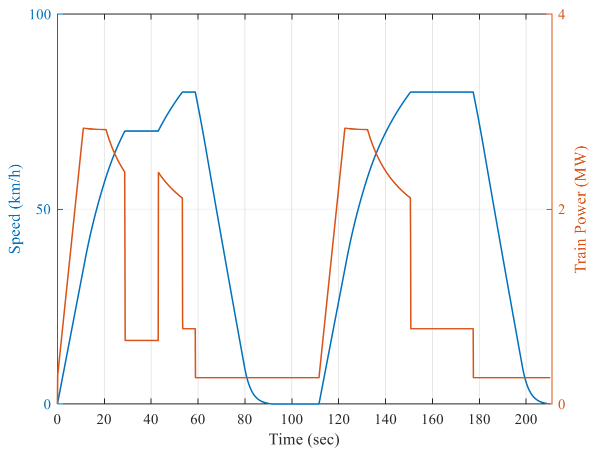


**Fig. 5. Train speed profile and consumed power of a train.**

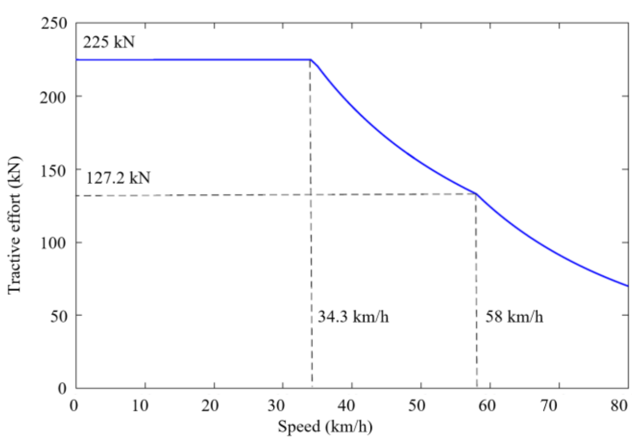


**Fig. 6. Tractive effort of the traction system.**

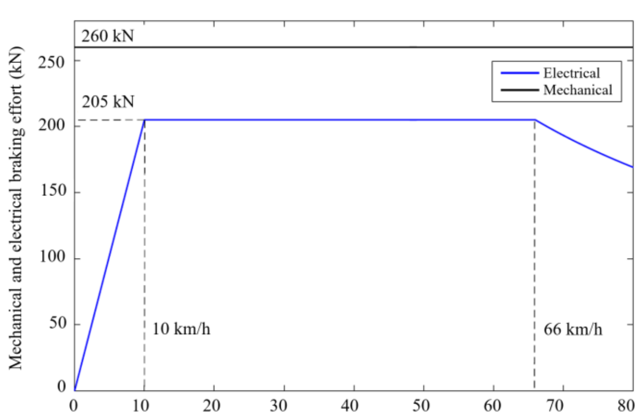


**Fig. 7. Brake effort of traction system.**

**Table 1. Vehicle data and electrical parameters**

| Category | Parameters/Value | |
|---|---|---|
| Operating Voltage | Train voltage | 750 V |
| Train Weight | Gross weight | 228 ton |
| Movement Feature | Max. vehicle speed<br>Max. acceleration rate<br>Max. deceleration rate | 80 km/h<br>0.87 m/s$^2$<br>1.00 m/s$^2$ |
| Train resistance | $A$ = 4025, $B$ = 118.67, $C$ = 0.871 | |
| Traction sub. 1&2 | No-load voltage<br>Rated power | 790 V<br>2550 kVA |
| 3rd-rail and Running rail | 3rd-rail resistance<br>Running rail resistance<br>Conductivity to earth<br>Earth resistance | 8.23 mΩ/km<br>72.83 mΩ/km<br>0.1 S/km<br>0.5 Ω |
| VLD parameters | Resistance (closed; open)<br>Trigger voltage | 0.001Ω ;100MΩ<br>±120 V |

### *3.2. Numerical results*

To study the effect of VLD operation on the rail potential and stray current at installed location of VLD, 3 factors are selected for the simulation i.e., time duration of VLD operation, variation of the running rail resistance and the ground resistance.

**Baseline Case: Considering the rail potential and stray current at the passenger station without VLD operation**

In the baseline case, the simulations are performed without operation of VLD to obtain the rail potential and stray current at the passenger station. The running rail resistance is in accordance with Table 1. The simulation results of the stray current and rail potential versus time are shown in Figs. 8 and 9, respectively.

From the simulation results, it was found that when the train starts to leave from station 2, if the VLD is not operated, the rail potential will exceed 120 V for 11.3 s. The peaks of rail potential and stray current at the station are around 138.2 V and 9.72 A, respectively.

**Case 1: Considering the effect of VLD duration of operation**

In this case, the simulations are performed in three different operating time durations of VLD: 10, 30, and 60 s. The simulation results of the stray current and rail potential versus time are shown in Fig. 10 and 11, respectively.

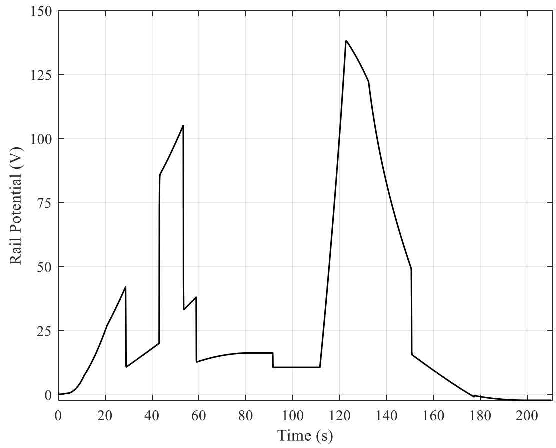


**Fig. 8. Rail potential versus time at the VLD installed location without VLD operation.**

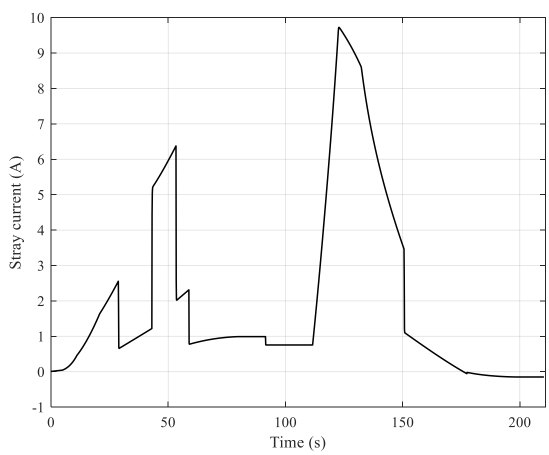


**Fig. 9. Stray current versus time at the VLD installed location without VLD operation.**

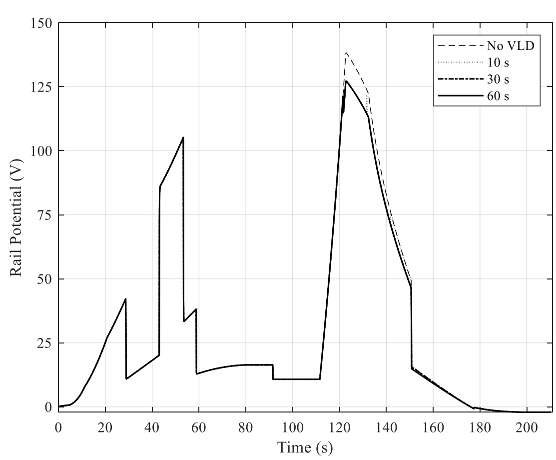


**Fig. 10. Rail potential versus time at the VLD installed location (considering the different VLD operating times).**

From the simulation results, it was found that when the train starts to leave from station 2, if the VLD is operated, the rail potential is suppressed depending on the operating time duration of VLD. When the time duration of VLD is less than the duration of overvoltage (e.g., time duration of VLD is set as 10 s), the rail potential is suppressed during the operating time of VLD, but the rail potential can shortly increase again after the VLD is turned off. During the VLD operation, the stray current considerably increases to approximately 262.5 A or 27 times of the baseline case (No VLD).

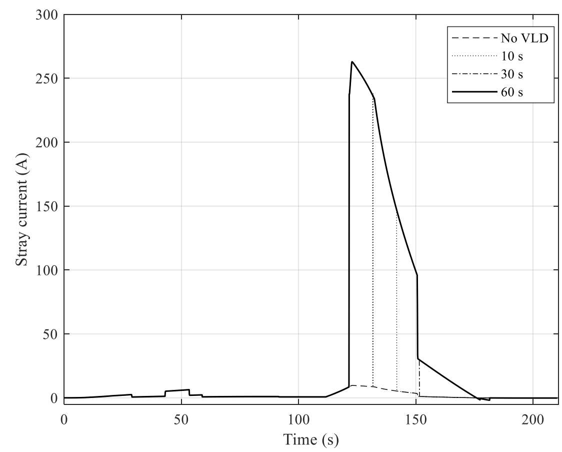


**Fig. 11. Stray current versus time at the VLD installed location (considering the different VLD operating times).**

### Case 2: Considering the effect of the running rail resistance

In this case, the different values of running rail resistance are considered as 80%, 100%, and 120% of the original value. The operating time of the VLD is set to 60 s. The simulation results of the stray current and rail potential are shown in Fig. 12 and 13, respectively.

When the rail resistance is reduced to 80%, the maximum rail potential is reduced by approximately 19% from the baseline case. If the running rail resistance is increased to 120%, the maximum rail potential is increased by about 26.7%, and the stray current is increased by 27.5%.

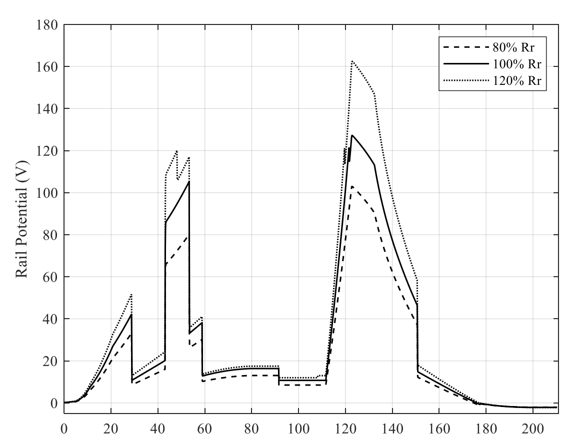


**Fig. 12. Rail potential versus time at the VLD installed location (considering the different running rail resistance).**

**Case 3: Considering the effect of the ground resistance**

In this case, the ground resistance of ground system at the station is considered as different values i.e., 80%, 100%, and 120% of the original value. The operating time of VLD is set at 60 s. The simulation results of the stray current and rail potential are shown in Figs. 14 and 15, respectively.

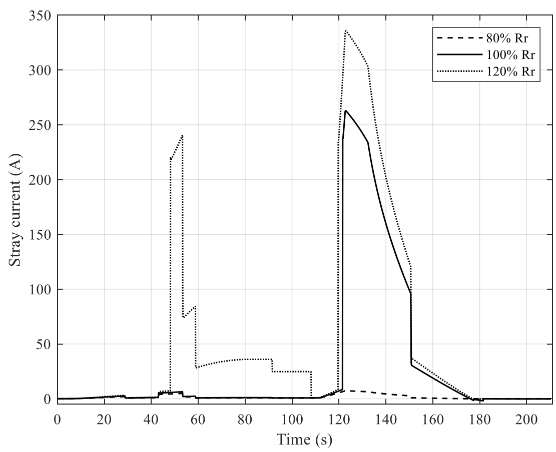


**Fig. 13. Stray current versus time at the VLD installed location (considering the different running rail resistance).**

When the ground resistance is changed, the rail potential is slightly changed. During the VLD operation, the rail potential with different ground resistance was approximately the same, but the stray current was considerably changed. From the results, when the ground resistance is reduced to 80%, the maximum rail potential is reduced by only around 1.97%, while the stray current is increased by 21.5%. When the ground resistance is increased to 120%, the peak rail potential increases by only approximately 1.34% and the stray current is reduced by 14.9%.

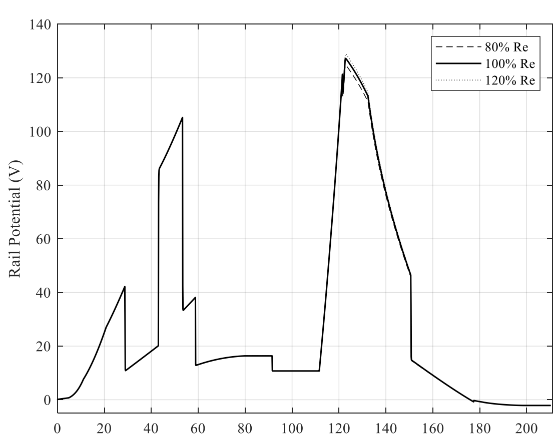


**Fig. 14. Rail potential versus time at the VLD installed location (considering the different ground resistance)**

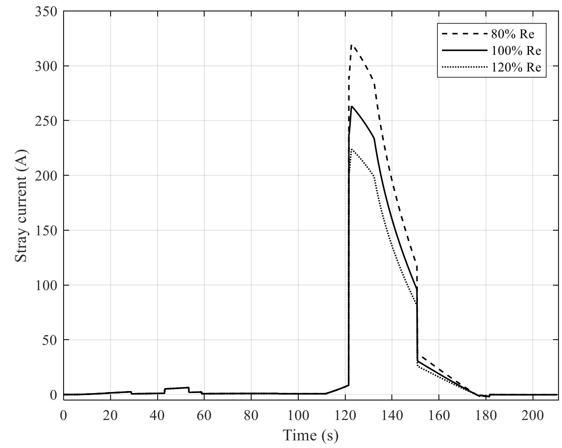


**Fig. 15. Stray current versus time at the VLD installed location (considering the different ground resistance)**

### *3.3. Discussion*

The operating time duration of the VLD directly affects the time duration for suppressing the rail potential, which exceeds the limit. The longer operating times allow the rail potential to be continuously controlled in the safety condition. An operating time that is too short will cause the VLD to operate intermittently. When the VLD is operated, the rails are directly connected to the ground system causing the very high stray current. Therefore, the operating time of the VLD is too long, the duration of the high stray current will be prolonged.

From the simulation results, it was found that the rail potential varies with the running rail resistance. When the running rail resistance increases, the rail potential increases resulting in considerable increase in the stray current. The ground resistance has a slight effect on the rail potential, but it still affects the stray current.

The variation of rail potential in normal operating condition is considered in this paper. However, in practical system, the rail potential can be raised to an abnormal value due to many reasons, e.g., switching operation, surge voltage due to lightning nearby area, induced voltage from nearby AC power line. To consider abnormal operation, the equivalent circuit model must be developed to represent specific events.

## 4. CONCLUSION

This paper presents the effect of operating the voltage limiting devices (VLD) installed at the passenger station to protect the passengers from the rising rail potential while the train is operating under normal conditions. For the simulation, the electrical model with lumped parameter is selected and developed for simulating the variation of rail potential and stray current. From the simulation results, it was found that the operating time of the VLD affects the continuity of the rail potential suppression. A large amount of operating time will cause excessive stray current for a long time. Therefore, an appropriate time should be considered from the time duration when the rail potential exceeds the predetermined value or safety value. In addition, the running rail resistance directly affects the rail potential, while the ground resistance slightly affects the rail potential, but it still has a considerable effect on the stray current.

For the further works, the effect of EMC is supposed to be included to demonstrate the case of induced voltage and current from nearby high voltage power line. However, the simulated model must be further developed for performing the EMC phenomenon due induction coupling between AC power line and DC feeding system.

## ACKNOWLEDGEMENTS

This research was funded by Thailand Science Research and Innovation Fund, and King Mongkut's University of Technology North Bangkok with Contract no. KMUTNB-MHESI-64-14.1.

## REFERENCES

[1] Kimura, S. Miyauchi, T. Oguma, K. Takahashi, H. and Teramura, K. 2020. Rail Potential Calculation Model for DC Railway Power Supply Equipped with Voltage Limiting Device. Proceedings of the European Conference on Power Electronics and Applications. Lyon, France, 7-11 September.

[2] IEC 62128-1. 2013. Railway applications – Fixed installations – Electrical safety, earthing and the return circuit – Part 1: Protective provisions against electric shock.

[3] EN 50122–1. 2011. Railway applications-fixed installations: electrical safety, earthing and the return circuit – Part 1: Protective provisions against electric shock, British Standards Institution.

[4] Richter, B. Bernhard, A. and Milutinovic, N. 2007. Protection against unacceptable voltages in railway systems. Proceedings of AusRAIL PLUS. Sydney, Australia, 4-6 November.

[5] Sim, W.M. Thong, M. and Chan, C.F. 2005. Touch voltage protection on Singapore MRT system. Proceedings of the International Power Engineering Conference. Singapore, 29 November-2 December.

[6] Mariscotti, A. 2021. Electrical safety and stray current protection with platform screen doors in DC rapid transit. IEEE Transactions on Transportation Electrification 7(3): 1724-173.

[7] Ibrahem, A. Elrayyah, A. Sozer, Y. and Abreu, A.D. 2015. DC railway system emulator for stray current and touch voltage prediction. Proceedings of IEEE Energy Conversion Congress and Exposition (ECCE). Montreal, QC, Canada, 20-24 September.

[8] Charalambous, C. Buxton, D. and Aylott, P. 2016. Practical Contemplation of Stray Current Calculation and Monitoring in DC Mass Transit Systems. IEEE Vehicular Technology Magazine 11(2): 24-31.

[9] IEC 62128-2. 2013. Railway applications-fixed installations: electrical safety, earthing and the return circuit –Part 2: Provisions against the effects of stray currents caused by D.C. traction systems.

[10] Du, G. Zhang, D. Li, G. Wang, C. and Liu, J. 2016. Evaluation of rail potential based on power distribution in DC traction power systems. Energies 9(9): 729.

[11] Lin, S. Zhou, Q. Lin, X. Liu, M. and Wang, A. 2020. Infinitesimal method based calculation of metro stray current in multiple power supply sections. IEEE Access 8: 96581-96591.

[12] Cotton, I. Charalambous, C. Aylott, P. and Ernst, P. 2005. Stray current control in DC mass transit systems. IEEE Transactions on vehicular technology 54(2): 722-730.

[13] Xu, S.Y. Li, W. and Wang, Y.Q. 2013. Effects of vehicle running mode on rail potential and stray current in DC mass transit systems. IEEE Transactions on Vehicular Technology 62(8): 3569-3580.

[14] Aatif, S. Hu, H. Rafiq, F. and He, Z. 2021. Analysis of rail potential and stray current in MVDC railway electrification system. Railway Engineering Science 29(4): 394-407.

[15] Sumpavakup, C. Mongkoldee, K. Ratniyomchai, T. and Kulworawanichpong, T. 2020. Touch and Step Voltage Evaluation based on Computer Simulation for a Mass Rapid Transit System in Thailand. International Journal of Intelligent Engineering and Systems 13(5): 159-169.

[16] Sumpavakup, C. Ratniyomchai, T. and Kulworawanichpong, T. 2017. Optimal energy saving in DC railway system with on-board energy storage system by using peak demand cutting strategy. Journal of Modern Transportation 25(4): 223–235.